JMEPEG (2010) 19:599–606
DOI: 10.1007/s11665-009-9513-8

1059-9495/$19.00

Cut Front Geometry Characterization in Cutting Applications of Brass with Abrasive Water Jet

Adnan Akkurt

(Submitted November 19, 2008; in revised form June 10, 2009)

Abrasive water jet (AWJ) cutting is an advanced manufacturing process for machining hard to cut materials. In this study, brass-353 samples of different thicknesses were cut by AWJ using different feed rates to identify the relationships between depth of cut (material thickness), feed rate, and deflection of cutting edge geometry. The effects of material thickness on the AWJ cut surface roughness were investigated and discussed. Deflection of cutting edge geometry in AWJ cutting process was assessed. Cutting edge geometry was characterized by analyzing the surface properties of cut samples.

Keywords abrasive water jet cutting, cutting front geometry, surface quality

1. Introduction

Abrasive water jet (AWJ) cutting is an advanced manufacturing tool that is used for machining hard to cut materials. There are essentially two types of water jets: pure water jet (WJ) and abrasive water jet (AWJ). The primary difference between the WJ and AWJ is the addition of an abrasive medium to increase the abrasive water jet cutting ability (Ref 1). WJ and AWJ cutting processes do not generate heat as other processes, so there are no heat-affected zones. This is useful for cutting materials for which heat may change their properties (Ref 2-7). To cut complex shapes with a variety of corners and curves, the feed rate must be carefully adjusted. Deflection of the jet causes increased taper, inside corner errors, and sweepings out of arc. AWJ cuts materials with feed rate of abrasive particles not pressure. The cutting power is obtained by means of a transformation of hydrostatic energy into a jet of a sufficient kinetic energy to disintegrate the material (Ref 1, 4-7). A schematic figure of water jet cutting system is given in Fig. 1. Cutting operations form a corner termed as "cutting front geometry." In the literature it is reported that stage formation in AWJ affects the cutting front geometry in AWJ cutting processes (Ref 8). Stages in cutting front geometry formation are given in Fig. 2. Energy losses during the cutting process with AWJ cause the cutting front geometry to be different from that of ideal geometry as shown in Fig. 3. A mathematical model of cutting front shown in Fig. 4 was developed by Momber (Ref 9). Experimental studies to concurrently find energy losses have shown that relative cutting depth ($\Phi(h) = h/h_{max}$) can be represented with an adjunct polynomial. It has been ascertained that regression parameters of these polynomials are independent of sample material and processing conditions. In this study, correlation coefficients could be determined from parabolic modeling, whereas equations to be used to predict energy losses were mathematically modeled. The starting point of mathematical model that Momber developed is based on parabolic of Fig. 8, which is obtained by comparing cutting front geometry during real operation and ideal cutting front geometry without any energy loss (Ref 9). This parabolic model was obtained by comparing the ideal cutting front geometry and ideal cutting front (Ref 8-12). Studies in the literature validate the parabolic model. Wang and Wong (Ref 13) have improved empirical models for kerf geometry, and quality is finally established for the prediction and optimization of AWJ cutting performance. Hlaváča et al. (Ref 14) have explained the relationship between the declination angle and cutting surface quality. Hascalik et al. (Ref 15) have examined the profiles of machined surfaces, kerf geometries, and microstructural features of the machined surfaces.

In this study, brass-353 samples of different thicknesses were cut by AWJ using different feed rates to identify the relationships between cutting front geometry and feed rate. The effects of thickness on the AWJ cut surface roughness were investigated and discussed. Deflection of cutting edge geometry in AWJ cutting process was assessed. Cutting front geometry was characterized by analyzing the surface properties of cut samples.

2. Experimental Work

Brass-353 material was cut with AWJ process using different feed rates. Brass is widely used in manufacturing industry. The nominal chemical composition of brass-353 is: 0.831% S, 2.21% Pb, 36.37% Zn, 0.216% P, 0.293% Fe, 0.442% Al, <59.23% Cu, and 0.237% Ni. In this study, sheet plates with thicknesses of 5, 10, 15, and 20 mm were cut with AWJ. Two different feed rates were used for cutting each of the thicknesses as shown in Table 1. First feed rate was recommended by manufacturer of AWJ system for the studied material. The second feed rate was arbitrarily selected as 20 mm/min for all samples. The other parameters in cutting processes were kept constant. The characteristics of AWJ

Adnan Akkurt, Faculty of Industrial Arts Education, Gazi University, 33480 Ankara, Turkey. Contact e-mail: aakkurt@gazi.edu.tr.

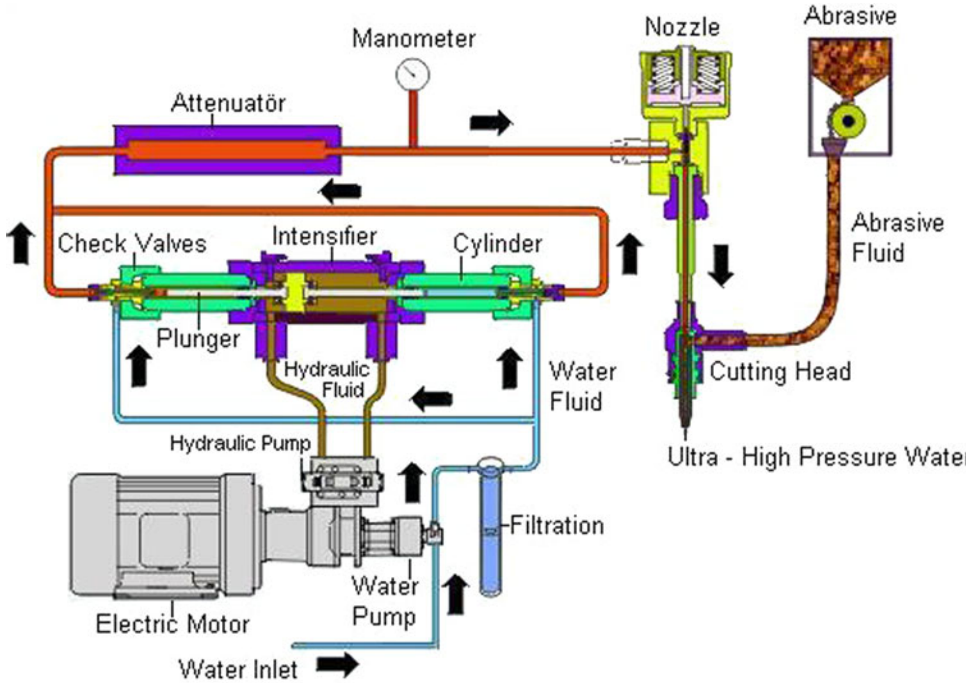

Fig. 1 Graphical simulation of WJ cutting system

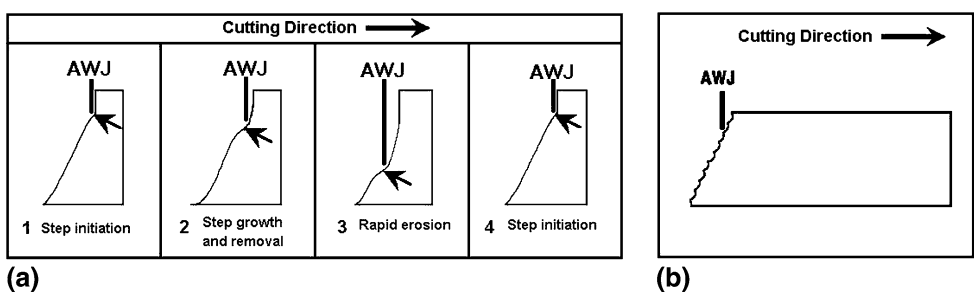

Fig. 2 Stage formation and depreciation in the cutting front section geometry (Ref 8)

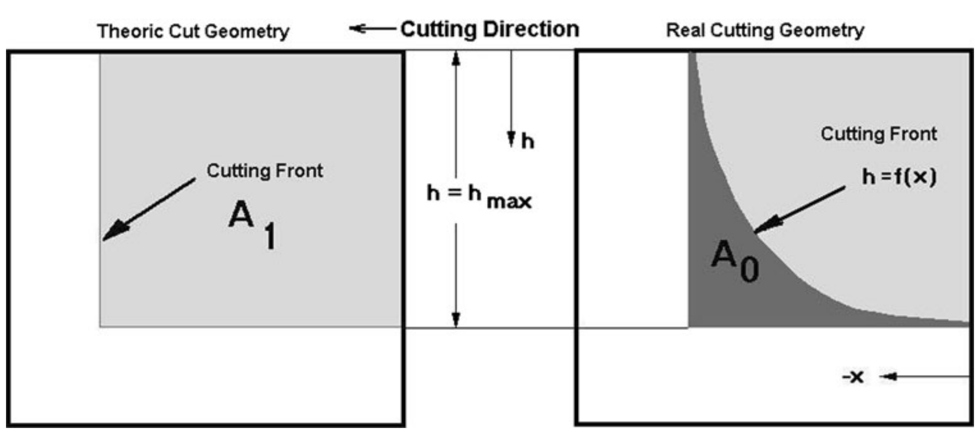

Fig. 3 Energy loss comparison between ideal cutting and actual cutting with AWJ (Ref 9)

system and cutting parameters are shown in Table 2 (Ref 1). "Rand" brand in the cutting operations of the material with AWJ was performed on Ingersoll Rand AWJ system. Surface roughness measurements of the cut surfaces were made using Mitutoyo Surface Analyzer 402 device. Surface hardness of workpieces was measured with Instron Wolpert Testor based on HV 30 value. Micrograph of the cut surfaces of samples were taken by Panasonic WVCP410 model type N334 microscope.

The samples were etched with 2 mL HNO_3 and 98 mL methanol mixture for 20 s. To identify cutting front geometry, two of the samples with the 10 and 20 mm thicknesses were cut by AWJ to half of their length. These samples were then separated (cut) with a milling machine to observe the cutting front geometry of AWJ. A relationship between the cutting depth (material thickness) and cutting front geometry was developed.

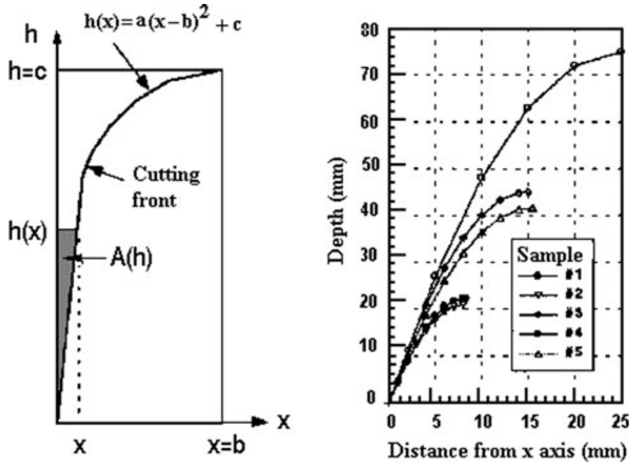

Fig. 4 Parabolic models of different materials in the processing by AWJ (Ref 9)

Table 1 Lateral improvement feed rate chosen in the cutting process based on material thickness

	5 mm		10 mm		15 mm		20 mm	
	a	b	a	b	a	b	a	b
Material	**Recommended and identified fixed feed rate, mm/min**							
Brass-353	R 140	I 20	R 63.16	I 20	R 39.62	I 20	R 28.46	I 20

3. Results and Discussion

When the samples were examined, it was observed that surface roughness had increased as the depth of cut (material thickness) was increased. This can be explained with the deformation of the sharp edges of the abrasive particles as illustrated in Fig. 5. Pressure loss occurs in the jet after contact with the material because of the friction of the abrasive particles with the abraded particles of the material. Cut surface topology of the studied brass-353 ($\alpha + \beta$ brass) was similar to that reported in the earlier studies on ductile aluminum (Ref 8, 16-22). The results show that there are two different wear mechanisms: cutting wear and abrasive wear for ductile and

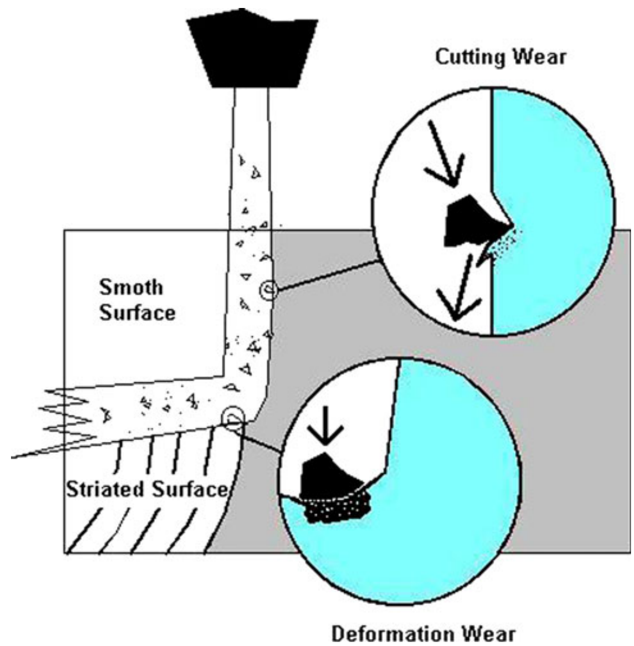

Fig. 5 Formation of different regions in AWJ cutting (Ref 1)

Table 2 Technical data on the abrasive water jet system and the pressure unit (Ref 1)

Cutting frame with the abrasive water jet and the pressure unit			
Orifice diameter	0.25 mm	Energy consumption	58 kWh
Pump capacity	3 L/min	The booster working pressure	Min 35 – Max 200
Water consumption	≈3.5 L/min	The pump piston diameter	20 mm
The temperature of the water used by the system	48 °C	The inlet pressure of water into the pressure booster	0.6 MPa
The working pressure of the booster	20 MPa	The inlet diameter of water into the nozzle	0.25 mm
The outlet pressure of water from the pressure booster	2 MPa	The inlet diameter into the abrasive nozzle	0.75 mm
Water flow rate	3 L/min	Stand-off distance	4 mm
The outlet velocity of water from the nozzle	800 m/s	Water pressure at the instance of discharge	400 MPa
Temperature at the instance of cutting	≈55 °C	Jet angle	90°
Current consumption during work	380 V	Electric engine capacity and consumption	22 kW, 58 kWh
The amount of abrader consumed	250 g/min	The material used in the nozzle head	Sapphire
The abrader used	GMA Garnet	Chemical composition	$Fe_2O_3Al_2(SiO_4)_3$
Abrasive hardness	7.5-8 Mohs	Abrasive particle size	300 μm
The pressure boost capacity	At a rate of 1/20	Nozzle length	76.2 mm
Abrasive water outlet diameter from the nozzle	1 mm	Garnet mesh number	80 Mesh
Slurry content	% 18	Mixing tube length	88.9 mm
Mixing tube diameter	1.27 mm	Orifice life	40-50 h

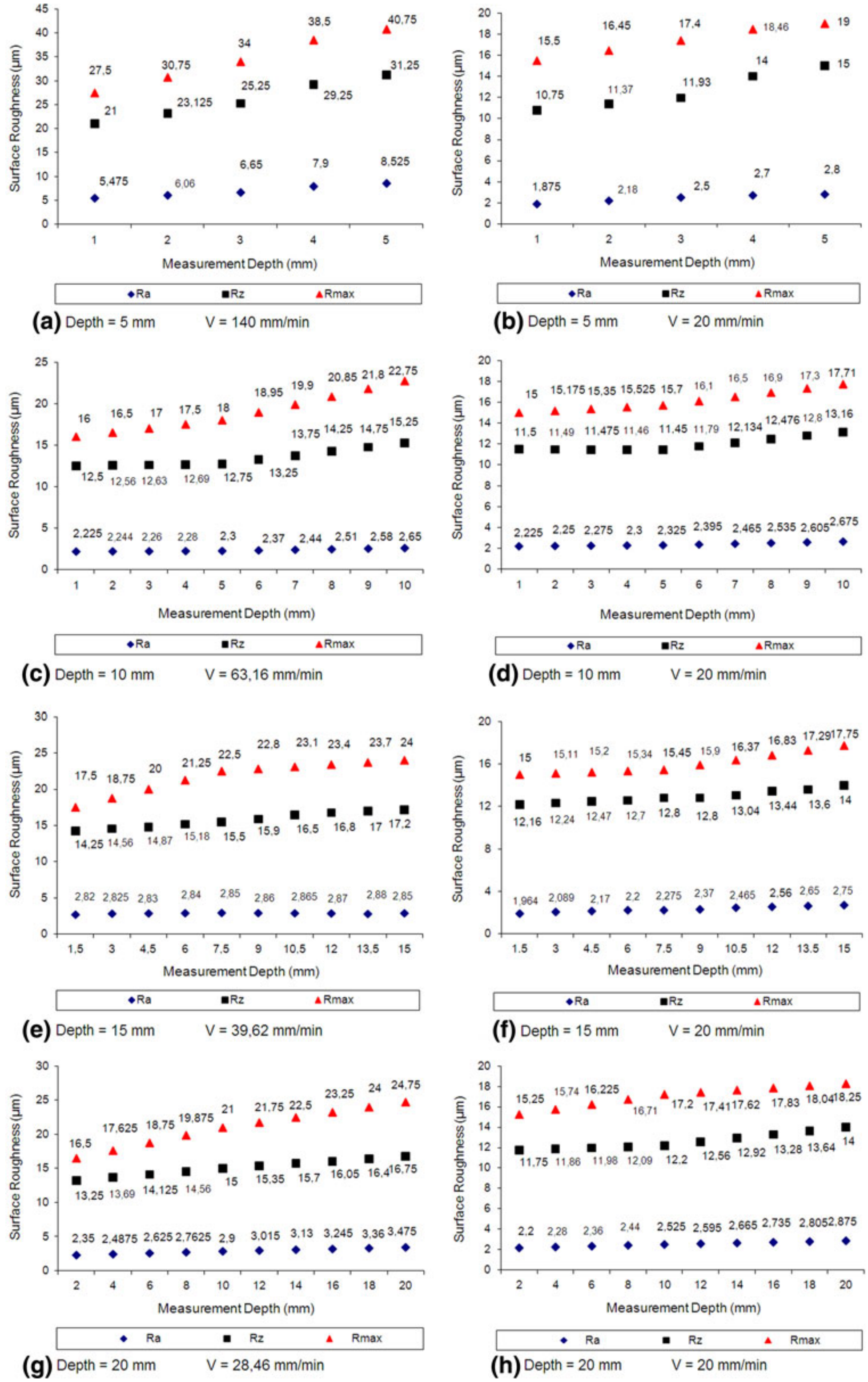

Fig. 6 Surface roughness obtained upon cutting Brass-353 at different lateral feed rates and depths of cut

fragile materials. Surface roughnesses of the samples with four different thicknesses that are cut with manufacturers'-recommended feed rate and fixed feed rate of 20 mm/min are given in Fig. 6(a, b) and 7(a, b), respectively. The surface roughness of the 5 mm samples was higher than that of the thicker samples. This result reveals that in AWJ cutting process, the pressure of the jet causes greater deformation as the thickness of the material reduces. When the cut surface was examined it was seen that the surface roughness and quality of the upper region of the cut surface was better than that of the lower region. These results reveal that cutting mechanism yields a better surface finish and quality than wear mechanism in AWJ cutting

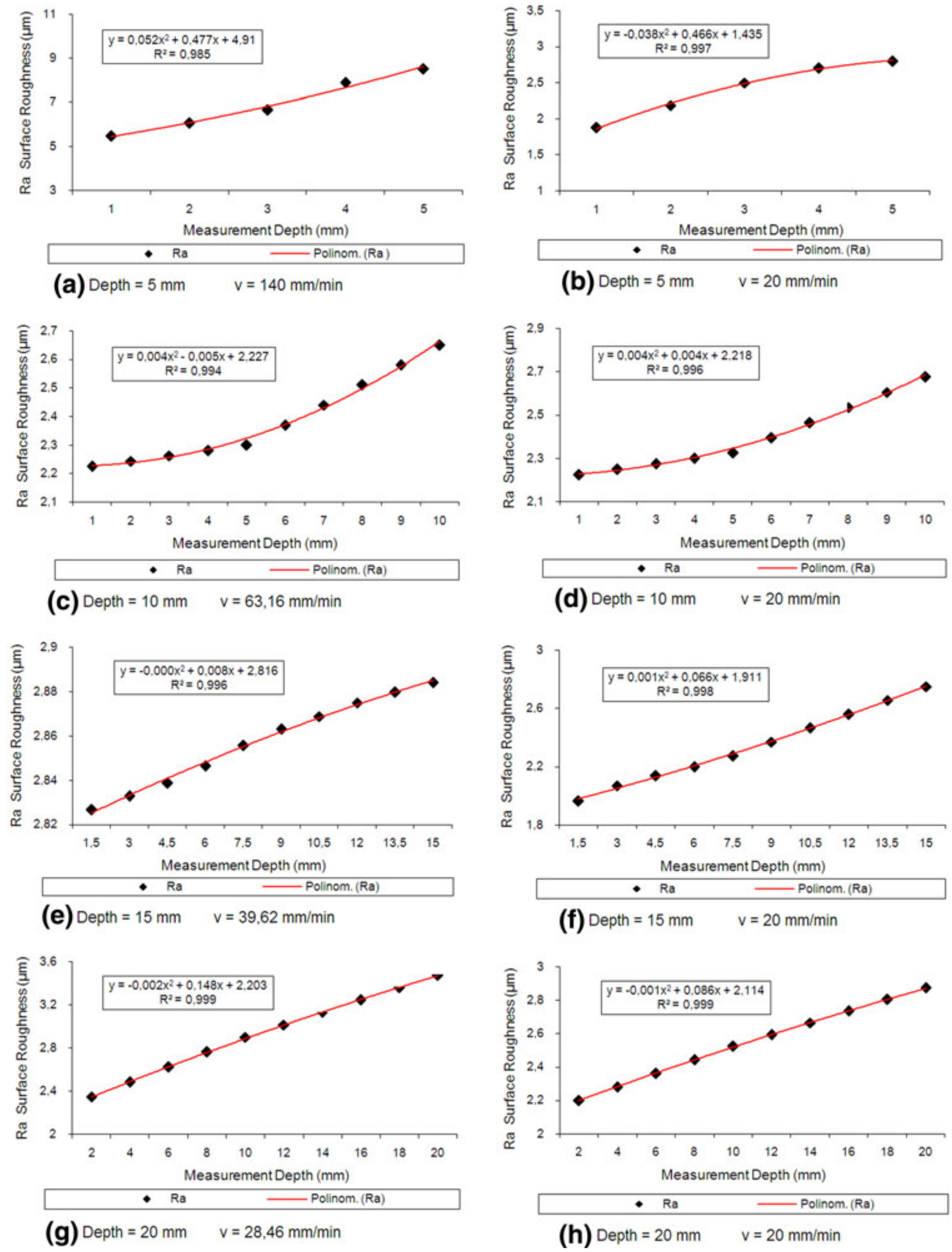

Fig. 7 Parabolic models for surface roughness values (*Ra*) in cutting Brass-353 at different lateral feed rates

applications. These results are in accordance with the literature (Ref 19, 23-33). Surface roughness values of different thicknesses are given in the Fig. 6.

The mean surface roughness (*Ra*) for the AWJ cutting of 5 mm thick brass-353 sample at the manufacturer-suggested feed rate of 140 mm/min was measured as 8.525 µm, and 2.8 µm for 20 mm/min feed rate. Moreover, surface roughness values found for the 5 mm thick samples are higher than those for 10, 15, and 20 mm thick samples. These results are in agreement with the studies in the literature which suggest that thin specimens should not be cut by AWJ (Ref 30, 31). Mean *Ra* values of the cut surfaces and second-degree polynomial equations of those values are shown in Fig. 7 for feed rate proposed by the manufacturer and the selected fixed feed rate. For all the thicknesses, it is seen that surface quality and roughness of the cut surfaces deteriorate as the depth of cut (material thickness) increases. From Fig. 7 it is seen that there is a significant difference between the results of surface roughness values obtained with the manufacturer-recommended feed rate of 140 mm/min and selected fixed feed rate of 20 mm/min for 5 mm thickness sample. Maximum surface roughness values were measured as 8.525 and 2.8 µm for feed rate of 140 and 20 mm/min, respectively, for 5 mm thickness. These results reveal that reducing the feed rate improves the surface quality and roughness in AWJ cutting processes. From Fig. 7 it is seen that reducing the feed rate from the manufacturer recommended value to 20 mm/min improves the surface roughness to a limited extent for 10, 15, and 20 mm thicknesses. These results show that there is a cutting range for materials in AWJ cutting process. The graph and equations characterizing mean surface roughness (*Ra*) in Fig. 7 subject to cross-section depth in AWJ cutting reveals the fact that they

Table 3 Equations and the coefficient of determination (R^2) characterizing mean surface roughness provided for different materials in different thickness measurements

Material	Thickness, mm	Lateral feed rate, mm/min	Equation(a)	Coefficient of determination (R^2)
Brass-353 (α + β)	5	140	$Ra = 0.0527x^2 + 0.4777x + 4.91$	0.9855
		20	$Ra = -0.0384x^2 + 0.4666x + 1.435$	0.9979
	10	63.16	$Ra = 0.0049x^2 - 0.0051x + 2.2276$	0.9947
		20	$Ra = 0.0043x^2 + 0.004x + 2.2188$	0.9962
	15	39.62	$Ra = -0.0002x^2 + 0.0085x + 2.8168$	0.9962
		20	$Ra = 0.0017x^2 + 0.0667x + 1.9112$	0.9983
	20	28.46	$Ra = -0.0021x^2 + 0.148x + 2.2031$	0.9998
		20	$Ra = -0.0011x^2 + 0.0865x + 2.1141$	0.9999

(a) Equation of average surface roughness

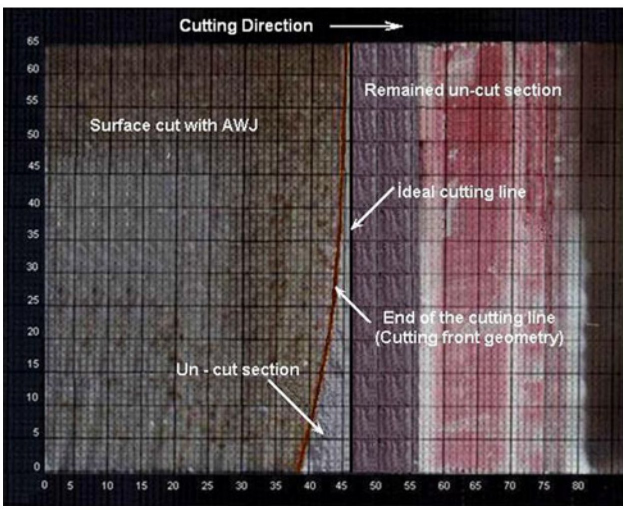

Fig. 8 Determination of cutting front section geometry separated from ideal geometry

may be characterized by a second-degree polynomial as a parabolic function. Nearly, in all the examined thicknesses, the coefficient of determination (R^2) is found to be greater than 0.99. Thus, for any depth level and feed rate it is possible to keep the surface roughness under control. In the equations, variable *Ra* corresponds to deviation from an ideal geometry and variable *x* corresponds to cutting depth (material thickness) in the form of second-degree polynomials. Equations and the coefficient of determinations for studied thicknesses of brass material (R^2) are given in Table 3.

Deflection from the ideal cutting geometry ("cutting front section geometry") is characterized in Fig. 8 in units of mm. To identify cutting front geometry, two of the samples with 10 and 20 mm thicknesses were cut by AWJ to half of their length. These samples were than separated (cut) with a milling machine to observe the cutting front geometry of AWJ. Those surfaces on which the final cutting line existed were magnified under an optical microscope and their images transferred to a millimeter segmented paper. Deviation from the ideal geometry was calculated and is plotted in Fig. 9 and 10. Graphs and equations characterizing the cutting front section geometry prove the fact that, during AWJ cutting operation, the cutting front section formed by deviation from the ideal geometry is possible and can be characterized by a second-degree polynomial as a

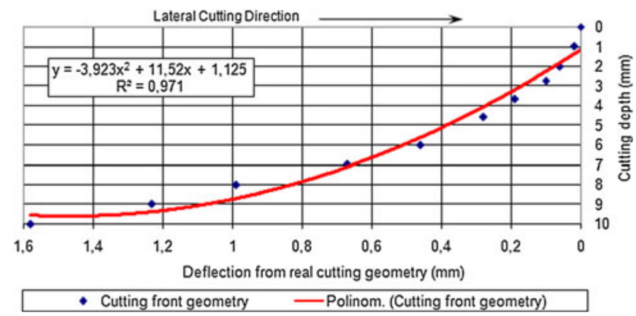

Fig. 9 Cutting front section geometry in 10 mm thick samples

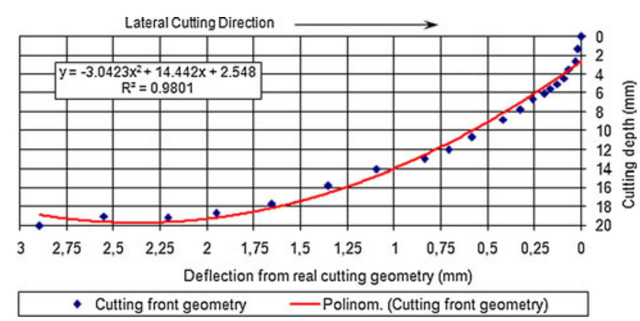

Fig. 10 Cutting front section geometry in 20 mm thick samples

parabolic function. For the studied brass samples, 10 and 20 mm thicknesses, the coefficient of determinations (R^2) were found to be over 0.99. These results are in agreement with the studies characterizing the cutting front section geometry in the literature (Ref 9, 34, 35). These values were used to model cutting front geometry mathematically by utilizing a parabolic function for studied brass material. The equations of cutting front geometry are given in Table 4. In the experimental study, no significant alterations are found in the metallurgic properties of the materials. The original microstructure, composed of alpha and beta phases, and the cut edge microstructure change after the cutting process is seen in Fig. 11. Because of the properties of cutting processes, deformation strain results in reduction in grain size, and failures in the microstructure are observed. Hardness measurements on the cut surface and base materials showed no variation between base materials and cut surface as seen in Table 5.

Table 4 Characterizing cutting front geometry, second-degree polynomial equations, and correlation coefficients

Material	Thickness, mm	Lateral feed rate, mm/min	Equation(a)	Correlation coefficient (R^2)
Brass-353 ($\alpha + \beta$)	10	63.16	$h = -3.9233x^2 + 11.529x + 1.1256$	0.9712
	20	28.46	$h = -3.0423x^2 + 14.442x + 2.548$	0.9801

(a) Equation of deflection from ideal cutting geometry. x = cutting depth (measured distance) and h = deflection from ideal cutting geometry

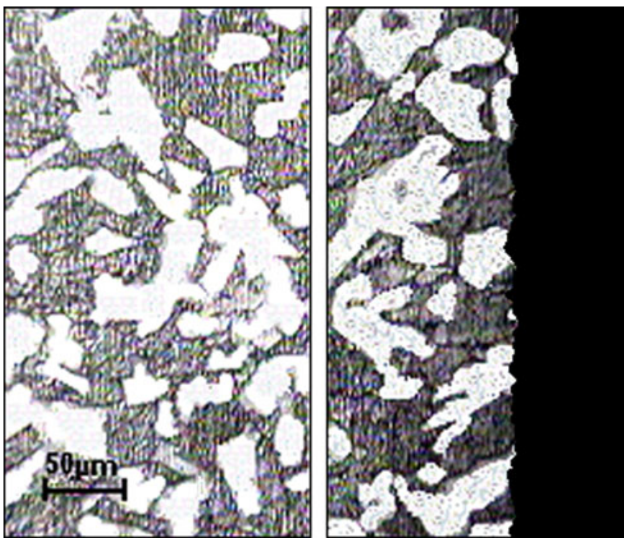

Fig. 11 Microstructure of Brass-353 material and cut section

4. Conclusion

From the results given above, the following conclusions can be drawn.

- In AWJ cutting process, the pressure of the jet causes higher deformation on thinner material. Reducing feed rate for thinner brass material results in better surface roughness value.
- The lateral deflection of jet changes due to material and cutting range. Reducing feed rate from upper limit to lower limit results in better surface roughness. These results are in line with current studies.
- Cutting mechanism gives better surface roughness and quality than wear mechanism in AWJ cutting applications.
- Surface quality and roughness of the cut surfaces deteriorate as the cutting depth increases.
- Mean surface roughness values (*Ra*) of brass material cut by AWJ are approximately around 2.65 and 3.475 μm.
- During AWJ cutting process, cutting front geometry is formed by deviation from the ideal geometry because of energy losses of the jet.
- Cutting front geometry caused by energy losses of jet and surface roughness of AWJ cut surfaces can be represented by a second-order parabolic function.

Acknowledgment

The authors thank Assab Korkmaz Celik Ve Isil İşlem AS for their valuable support to experimental studies.

Table 5 Hardness variations of brass materials after and before cutting by AWJ

Hardness	Brass-353
Base material	115.20 HV
Cut surface	118.50 HV

References

1. A. Akkurt, "Çesitli Malzemelerin Asındırıcı Su Jeti Ile Kesilmesinde Yüzey Özellikleri, Sertlik ve Mikro yapı Değisimlerinin Farklı Kesme Yöntemleriyle Karsılastırmalı Olarak Incelenmesi," Doktora Tezi, G.Ü. Fen Bilimleri Enstitüsü, Ankara, 2002, s 50–62
2. M. Hashish, Optimization Factors in Abrasive-Waterjet Machining, *J. Eng. Ind.*, 1991, **113**, p 132–139
3. H.J. Warnecke and M. Schlatter, Treatment of Materials with High Pressure Water Jets, E330, Vol. 60 (Stuttgart, Germany), 1984, p 189–201
4. W. Hunziker, *Water-Jet Cutting*, Bqstronic Lazer AG, Niederönz, Switzerland, 1990, p 12–17
5. F. Richard, *Waterjet Machining in Relationship to Design Engineering for Manufacturability*, Hydro-Abrasive Machining, Los Angeles, CA, 1992, p 60–67
6. A.W. Momber, R. Kovacevic, R. Schüneman, et al., The Influence of Abrasive Grain Size Distribution Parameters on the Abrasive Water Jet Machining Process, *Proceedings of the 25th NAMRI Conference*, K.P. Rajukar, Ed. (Dearborn, MI), Society of Manufacturing Engineers, 1996, p 21–26
7. M. Hashish, Precision Machining with Abrasive Water Jets, *Proceedings of the 6th American Water Jet Conference* (Houston, TX), 1991, pp 20–32
8. L. Ohlsson, J. Powell, and C. Magnusson, Mechanisms of Striation Formation in Abrasive Waterjet Cutting, *Proceedings of the 12th International Conference On Jet Cutting Technology*, Oct 25–27, 1994 (Rouen, France), 1994, p 151–164
9. A. Momber, A Simplified Mathematical Energy Dissipation Model for Water Jet and Abrasive Water Jet Cutting Processes, *8th American Water Jet Conference*, Aug 26–29, 1991 (Houston, TX), 1991, p 829–843
10. A. Momber and R. Kovacevic, Calculation of Exit Jet Energy in Abrasive Water Jet Cutting, *Manufacturing Science and Engineering*, ASME, New York, 1994, p 361–366
11. M. Hashish, Prediction Models for AWJ Machining Operations, *7th American Water Jet Conference*, Aug 28–31, 1993 (Seattle, WA), 1993, p 205–216
12. J. Chao and E. Geskin, Experimental Study of the Striation Formation and Spectral Analysis of the Abrasive Waterjet Generated Surfaces, *7th American Water Jet Conference*, Aug 28–31, 1993 (Seattle, WA), 1993, p 27–41
13. J. Wang and W.C.K. Wong, A Study of Abrasive Waterjet Cutting of Metallic Coated Sheet Steels, *Int. J. Mach. Tools Manuf.*, 1999, **39**, p 855–870
14. L.M. Hlaváča, I.M. Hlaváčová, L. Gembalová, et al., Experimental Method for Investigation of the Abrasive Water Jet Cutting Quality, *J. Mater. Process. Technol.*, 2009. doi:10.1016/j.jmatprotec.2009.04.011
15. A. Hascalik, U. Çaydaş, and H. Gürün, Effect of Traverse Speed on Abrasive Waterjet Machining of Ti–6Al–4 V Alloy, *Mater. Des.*, 2007, **28**, p 1953–1957

16. A. Momber, *Handbuch druckwasserstrahl-technik*, Beton Verlag GmbH, Düsseldorf, 1993, p 26–34
17. M. Niu, Y. Fukunishi, and T. Sawamura, Control of Striated Roughness on the Surface Cut by Abrasive Water Jet, *BHR Group Jetting Technology*, Ishinomaki Senshu University, Japan, 1996, p 769–777
18. P.L. Singh, W.L. Chen, and I. Munoz, Comprehensive Evaluation of Abrasive Waterjet Cut Surface Quality, *6th American Water Jet Conference*, Aug 26–27, 1991 (Houston, TX), 1991, p 139–161
19. L. Murugesh, S. Srinivasan, and R.O. Scattergood, Models and Materials Properties for Erosion of Ceramics, *J. Mater. Eng.*, 1991, **13**(11), p 55–61
20. S.L. Engel and T.J. Labus, Industrial Applications and Comparison of Laser and Abrasive Waterjet Technologies, *Fluid Jet Technology – Fundamentals and Applications*, 2nd ed., WJTA, St. Louis, 1993, p 12–18
21. A. Akkurt, Effect of Cutting Speed on Surface Roughness in AWJ Cutting Applications of Commercial Pure Aluminum and Al-6061 Aluminum Alloy, *J. Polytech.*, 2005, **8**(1), p 69–79
22. Y. Fukunishi, R. Kobayashi, and K. Uchida, Numerical Simulation of Striation on Water Jet Cutting Surface, *Proceedings of 8th American Water Jet Conference*, Aug 26–29, 1995 (Houston, TX), 1995, p 157–169
23. J. Zeng, R. Hines, and T.J. Kim, Characterization of Energy Dissipation Phenomena in Abrasive Water Jet Cutting, *Proceedings of the 6th American Water Jet Conference*, Aug 26–27, 1991 (Houston, TX), Water Jet Technology Association, 1991, p 163–177
24. D.K.M. Tan, A Model for the Surface Finish in Abrasive Waterjet Cutting, *Proceedings of 8th International Symposium on Jet Cutting Technology* (Durham, England), 1986, p 31–38
25. M. Hashish, Steel Cutting with Abrasive Water Jets, *Proceedings of 6th International Symposium on Jet Cutting Technology*, University of Surrey, UK, 1982, Paper K3
26. N.S. Guo, H. Louis, and G. Meier, et al., Recycling Capability of Abrasive Water Jet Cutting, in *Jet Cutting Technology*, A. Lichtarowicz, Ed., et al. Kluwer Academic Publishers, Dordrecht, 1992, p 503–523
27. R. Kovacevic, Surface Texture in Abrasive Waterjet Cutting, *J. Manuf. Syst.*, 1991, **10**(1), p 32–40
28. B.L. Liu, Y. Shang, and H. Yao, The Recent Premajet Advance in Cutting and Derusting Technology, in *Jet Cutting Technology*, A. Lichtarowicz, Ed., et al. Kluwer Academic Publishers, Dordrecht, 1992, p 451–460
29. W.L. Chen and E.S. Geskin, Measurements of the Velocity of Abrasive Waterjet by the Use of Laser Transit Anemometer, in *Jet Cutting Technology*, D. Saunders, Ed., Elsevier, London, 1991, p 23
30. H. Nakamura, T. Nazaraki, and S. Yanagihara, Cutting Technique and System for Biological Shield, *Nucl. Technol.*, 1989, **86**, p 168–178
31. M. Mozurkiwicz, L. Fincuan, and R. Ferguson, Investigation of Abrasive Cutting Head Internal Parameters, *Proceedings of the 9th International Symposium on Jet Cutting Technology*, P.A. Woods, Ed., BHRA Fluid Engineering, Cranfield, England, 1988, p 34–37
32. M. Hashish, Visualization of the Abrasive-Waterjet Cutting Process, *Exp. Mech.*, 1988, **28**(2), p 159–169
33. R. Kovacevic, R. Mohan, and H.E. Beardsley, Monitoring of Thermal Energy Distribution in Abrasive Waterjet Cutting Using Infrared Thermography, *ASME J. Manuf. Sci. Eng.*, 1996, **118**(4), p 555–563
34. A.W. Momber, R. Kovacevic, R. Kwak, and R. Mohan, Experimental Estimation of Energy Dissipative Processes in Work Pieces During Abrasive Water Jet Cutting, *8th American Water Jet Conference*, Aug 26–29, 1995 (Houston, TX), 1995, p 26–29
35. A. Momber, Schneidversuche an stahlbeton mit dem abrasivdruckwasserstrahlen, *On und Stahlbetonbau*, 1994, **89**, p 132–134